Structural Characterization of a Novel Catalyst Obtained from Nanoscopic $NiAl_x$ by X-ray Absorption Spectroscopy

H. Modrow,*,† M. O. Rahman,† R. Richards,‡ J. Hormes,§ and H. Bönnemann||

Physikalisches Institut der Universität Bonn, Nussallee 12, 53115 Bonn, Germany, International University Bremen, Campus Ring 8, 28759 Bremen, Germany, Center for Advanced Microstructures and Devices, 6980 Jefferson Highway, Baton Rouge, Louisiana 70806, and MPI für Kohlenforschung, Kaiser-Wilhelm-Platz 1, D-45470 Mülheim an der Ruhr, Germany

Received: December 31, 2002; In Final Form: August 25, 2003

Information on geometric and electronic structure of a promising novel $NiAl_x$ catalyst is presented. It is based on the analysis of both X-ray absorption near edge (XANES) and extended X-ray absorption fine structure (EXAFS) data measured at the Ni K-edge of the catalyst, its precursor materials, and conventional Raney Nickel samples. The interpretation of these results is supported by real space full multiple scattering calculations using the "FEFF-8" code. In contrast to standard Raney Nickel, the new material cannot be described assuming a pure Ni-based sponge structure. Instead, although direct Ni−Ni bonds are observed, there is also a considerable amount of Ni−Al bonds remaining in the sample even after the leaching process is completed. This finding can tentatively be related to the nanoscopic nature of the catalyst.

Introduction

Some of the commercially most important types of catalysts used today for a wide range of applications are of Raney-type. This class of catalysts, which is also referred to as "skeletal" or "sponge" catalysts, was created by Murray Raney by NaOH-leaching of NiSi- and NiAl-alloys, respectively.[1,2] Since then, a vast amount of research has been performed on this class of materials. Still, it remains in the focus of scientific activity aiming for new applications,[3−6] improving the catalysts or finding improved reaction partners and conditions,[7−10] and better understanding of the materials, especially the modifications during the leaching process and their catalytic activity.[11−15] Although the class of the catalyst is defined relating to its geometric structure, it has been shown that in numerous cases[11,12,15] modification of its electronic structure, e.g., by addition of a few percents of a second transition metal, can influence its catalytic activity considerably. Consequently, it is essential to elucidate both the geometric and electronic structures to achieve a complete understanding of this type of catalyst.

Recently, Richards et al.[16] have described a "bottom up" preparation of nanoscale skeletal nickel catalysts based on a novel, wet chemical approach to the production of NiAl[17] that shows promising catalytic activity. Preliminary examination of the catalyst produced by leaching the $NiAl_3$ precursor prepared using this "bottom up" approach demonstrated a 4-fold increase in activity for the hydrogenation of butyronitrile.[16] Along with the possibility to vary over a broad range the Al-content of the intermediate $NiAl_x$ ($1 < x < 3$) from which the catalyst is then obtained by leaching, comes the possibility to fine-tune the catalytic activity. To make use of this chance, however, the exact understanding of this material is crucial. A direct attempt to obtain this understanding using nitrogen adsorption, TEM, elemental analysis, and X-ray diffraction (XRD)[16] provided only limited structural information. To illustrate this, XRD spectra of the activated catalyst investigated in this study and an activated Raney Nickel catalyst are displayed in Figure 1. The failure of these experimental approaches is due to two reasons. First, owing to the nanoscopic structural building blocks of the catalyst, only broadened peaks are obtained in the XRD spectrum. Second, the XRD signals of several phases which might possibly be present parallel to each other in the sample are separated by rather small angular differences, so that their unambiguous identification is not possible. Apart from that, XRD is inherently insensitive to areas in the particle in which the long-range order is disturbed.

Over recent years, X-ray absorption spectroscopy (XAS) has been shown to provide excellent information on nanoscopic systems[18,19] and their synthesis,[20] as this spectroscopic technique does not require—in contrast to diffraction techniques—long-range order in the sample.

In this technique, the energy dependence of the photoabsorption coefficient is measured in the vicinity of the ionization edge of the element of choice. At photon energies above the ionization edge, this leads to the creation of a photoelectron wave, which in turn undergoes scattering processes with the neighboring atoms, leading to an energy-dependent "interference pattern". The analysis of the extended X-ray absorption fine structure, i.e., the "interference pattern" at photoelectron energies where it is dominated by single scattering processes, allows for the analytical extraction of bonding distances, number, and type of neighboring atoms within the first few shells around the atom type selected by choosing the absorption edge that is measured.[21] Further information is accessible by interpreting the X-ray absorption near-edge structure which consists of two parts: (1) the energy region directly above the ionization edge which is dominated by multiple-scattering processes of the photoelectron and thus highly sensitive with respect to the coordination geometry of the absorber atom; (2) the energy region below the ionization edge, where transitions into unoccupied bound

* Corresponding author. E-mail: modrow@physik.uni-bonn.de.
† Physikalisches Institut der Universität Bonn.
‡ International University Bremen.
§ Center for Advanced Microstructures and Devices.
|| MPI für Kohlenforschung.

10.1021/jp022662b CCC: $25.00
Published on Web 10/10/2003

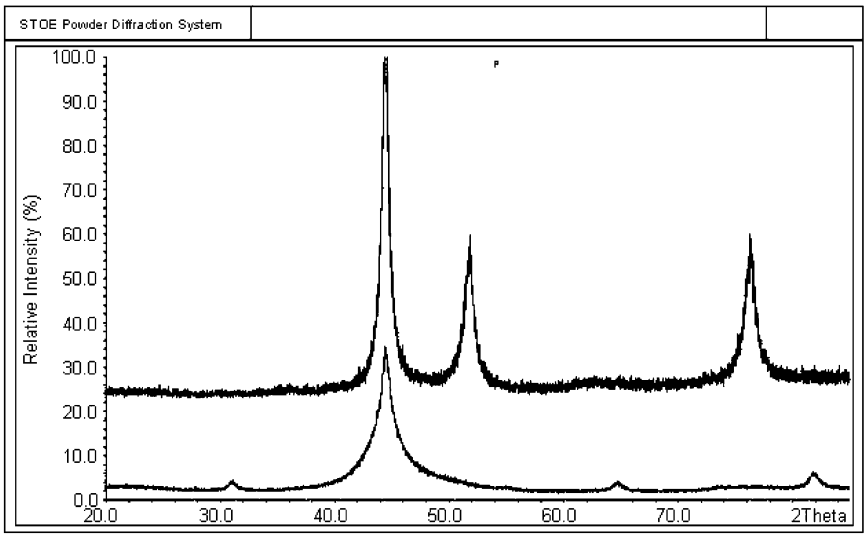

Figure 1. XRD spectra of activated novel calatyst (bottom) and activated Raney Nickel.

electronic states occur. Even when just relying on a fingerprinting approach, i.e., the comparison to reference spectra, these electronic transitions provide information on formal valency, electron affinity, ionicity, and effective atomic charges of the neighboring atoms and often also the symmetry of an atomic environment are obtained.[22−26] If several phases are present simultaneously in the sample, it is often possible to quantify their relative occurrence in the sample.[27,28] Even more detailed is the information which can be extracted from the near-edge spectra if it is possible to correlate it with calculations of the electronic structure.[29,30]

Experimental/Calculations

The method for the production of the $NiAl_x$ is described in detail elsewhere.[16,17] This method consists of the reaction between $Ni(COD)_2$ (where COD = cycloocta-1,5-diene) and $Al(ethyl)_3$ in toluene which leads to a black-brown dispersion. The educts for all reactions can be obtained, for example, from Alfa Aesar. Hydrogen is used in this reaction as a means to hydrogenate the olefinic compounds of COD and ethylene. Drying under vacuum and heat treatment (130 °C) under a hydrogen pressure of 50 bar yields a black powder which consists of nickel aluminide. The particles were found to form aggregates of 100−500 nm that were constituted of smaller particles of 5−7 nm (XRD via Scherrer equation) and 2−5 nm (TEM).

$$Ni(COD)_2 + xAlEt_3 \xrightarrow[\text{toluene}]{H_2} NiAl_x + \text{cyclooctane} + \text{ethane} \xrightarrow[16\text{ h, }130\text{ C}]{H_2} NiAl_x$$

Altering the stoichiometric ratios of the starting materials ($Ni(COD)_2$ and $Al(Et)_3$) facilitated the preparation of samples with Al/Ni ratios in the range from 1 to 3. The active skeletal catalysts were obtained by leaching the nickel aluminide with an excess of 5 M NaOH, decanting and drying under vacuum. All steps in the catalyst preparation and handling were done using air-free techniques. The leaching and washing steps were done using degassed UHQ water.

As a reference material for this study, commercial Raney Nickel (type 4200 obtained from Aldrich as an already activated sample stored under water) was used.

Sample preparation for the X-ray absorption spectroscopy measurements was performed under argon in a glovebox. The sample material was carefully ground, smeared in an even, thick layer on sticky Kapton foil, and sealed using a second layer of foil. The resulting "package" was finally fixed on a special sample holder for air- and moisture-sensitive samples described in detail elsewhere,[18] so that inert conditions were maintained throughout the transfer to the measurement chamber.

The experimental data presented in this study were taken in transmission mode at beamline "BN3" of the Electron Stretcher and Accelerator (ELSA) in Bonn, Germany, which was operating in 2.3 GeV mode during the measurements. To monochromatize the incoming radiation, a modified Lemonnier-monochromator[31] was used, which was equipped with Ge220 crystals ($2d$ = 0.40 nm [32]). For the detection of the incoming and transmitted beam, ionization chambers operated at 200 V and filled with 300 mbar of argon were used. Details about the used readout-electronics can be found in a previous study.[19] During the EXAFS measurements, the photon energy was scanned between 8050 and 9200 eV in steps of approximately 1.5 eV, with integration times of 1.5 s per point. The XANES data were taken in steps of approximately 0.8 eV, using integration times of 500 ms per point.

For the evaluation of the EXAFS spectra, the "UWXAFS" program package was used.[33−35] Fits were performed on the k-range between 2 and 10 with k^3-weight and an r-window of 1.25−2.8 Å. Fixing the coordination number for a 99.9% Ni foil obtained from "The EXAFS company" to 12 yields a S_0^2 value of 0.78, which was used for all the fits.

XANES data processing consisted of subtraction of a linear background fit to the preedge, followed by energy calibration relative to the first inflection point of a Ni foil, which was set to a photon energy of 8333 eV,[32] and normalization to an edge jump using the atomic background function obtained from the "UWXAFS" background subtraction tool "autobk".

For the calculations presented in this study, the "FEFF-8"-code, described in detail by Ankudinov et al., was applied.[36] It uses a Greens-function approach for a cluster-based, real space full multiple scattering calculation. This approach is extremely well suited to describe the absorption spectra as a function of a given cluster with a well-defined geometric environment, and it allows for a detailed interpretation of the electronic structure based on the l-projected density of state (lDOS),[26,29,30] although

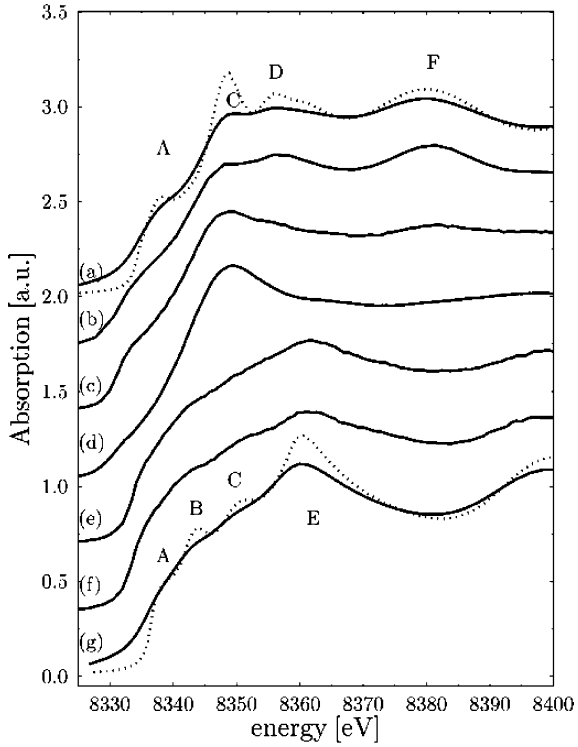

Figure 2. (top to bottom): XANES spectra of (a) Ni (theory) with (solid) and without (dotted) 2 eV broadening, (b) Ni foil, (c) commercial Raney Nickel, (d) new catalyst, (e) precursor material, (f) nanoscale NiAl reference, and (g) NiAl (theory)) with (solid) and without (dotted) 2 eV broadening.

it tends to slightly underestimate the intensity of resonances in the direct vicinity of the main absorption edge.

Results and Discussion

This section will start with the qualitative comparison—the interpretation of the XANES features which are labeled in Figure 2 is discussed in detail below—of the Ni K-XANES spectra of a Ni foil (b) and activated conventional Raney Nickel (c) displayed in Figure 2. Whereas there are clear differences between both spectra in the region near the absorption edge, the so-called "white line" region, which reflects the electronic structure, one clearly observes a perfect agreement of the phases of the shape resonances, indicating a similar structural environment of the absorbing atom.

Also shown in Figure 2 are the Ni K-XANES spectra of the catalyst after (d) and before (e) leaching as well as the nanoscale NiAl reference material (f). The spectra of the NiAl reference material (also referred to as "NiAl" below) and the $NiAl_x$ catalyst before leaching (also called "precursor material" below) are almost identical. The XANES spectrum of the activated catalyst after the leaching process clearly differs from both classes of material discussed so far. Evidently, although the leaching process leading to the optimum of activity is completed, the electronic structure of its final product is not equivalent to the commercial Raney Nickel catalyst.

The classification of the different materials described above on the basis of their electronic structure is confirmed by comparison of their EXAFS data displayed in Figure 3. Whereas a high degree of similarity between the NiAl reference and the precursor on one hand and of Ni foil and Raney Nickel on the other hand is evident from the comparison of their respective chi (κ) functions (i.e., the respective "interference patterns"), the completely different geometric environment of the Ni absorber atoms in the activated catalyst leads to a characteristic structure dominated by two peaks, which are not fully separated. It should be noted at this point that this structure cannot be reproduced by a superposition of the two types of interference patterns, which shows that we are not dealing with a mixture of these two phases. A similar, but more pronounced structure has been discussed previously in terms of these characteristic changes in two previous studies on transition metal-substituted nickel aluminides,[37,38] in which it could be linked to the presence of transition metal atoms on Al sites in the NiAl lattice. It is possible to correlate the fact that the structure is present, but not fully separated for the catalyst investigated in this study to the presence of Ni on both Ni and Al sites.

Before beginning a more detailed interpretation of these observations, we refer to the excellent agreement between the experimental data and the theoretical calculations performed in this study, using calculated and measured Ni K-XANES spectra of Ni (Figure 2a,b) and NiAl (Figure 2f,g), which are the only spectra for which independently determined structural information is available as examples. Consequently, these calculations provide a solid basis for the interpretation of the electronic structure information contained in the Ni K-XANES. Evidently, in both calculations, apart from the mere reproduction of the absorption spectrum, the direct assignment of the spectral features marked in Figure 2 to different structures in the lDOS is possible, as shown in Figure 4. As it is to be expected due to the dipole selection rule, the spectra can be described completely on the basis of the structures visible in the pDOS. Comparing, e.g., the Ni-projected pDOS of states for NiAl and Ni, respectively, it is evident that structure B is related to a Ni−Al bond with strong p character, as it emerges from a hybridization of Ni and Al pDOS with only slight admixture of sDOS. As a consequence, structure C, which is also related to this type of orbital, is reduced in intensity if Ni−Al bonds are present (as the total number of l-projected states is, of course, a constant). The strong Al dDOS (!) contribution to structure E strongly suggests that one is dealing with a structure which depends on a multiple scattering process rather than one to which a molecular orbital approach is suited. If this is the case, the same must be true for structure D, which is then related to Ni−Ni multiple scattering. Last but not least, it is interesting to discuss in some detail structure A, which is present in both spectra. In both cases, it emerges from Ni spd-hybridization, but it is important to note that if Al is present, its maximum is shifted to slightly lower energies.

Having reached a detailed understanding of the structures present in the XANES spectra, we turn to the discussion of the spectrum of the commercial catalyst. As mentioned above, the agreement of the phase of the shape resonances in the postedge region of the XANES spectra of bulk Ni and Raney Nickel is observed (see Figure 2). This clearly suggests a structural similarity between both materials. The reduced amplitude of the shape resonances and especially of the multiple scattering resonance D can be attributed to a higher degree of disorder in the Raney Nickel sample and a reduction of Ni nearest neighbor atoms. In fact, the EXAFS analysis (Table 1) using a value of $S_0^2 = 0.78$ agrees perfectly with this interpretation: in these two cases, Ni−Ni distances of 248 ± 1 pm and 251 ± 2 pm, respectively, are obtained, but the coordination number in commercial Raney Nickel is reduced to a value of 6.6 ± 1 compared to 12 obtained for the foil. The above-described structural results agree well with those obtained in previous studies.[39,40]

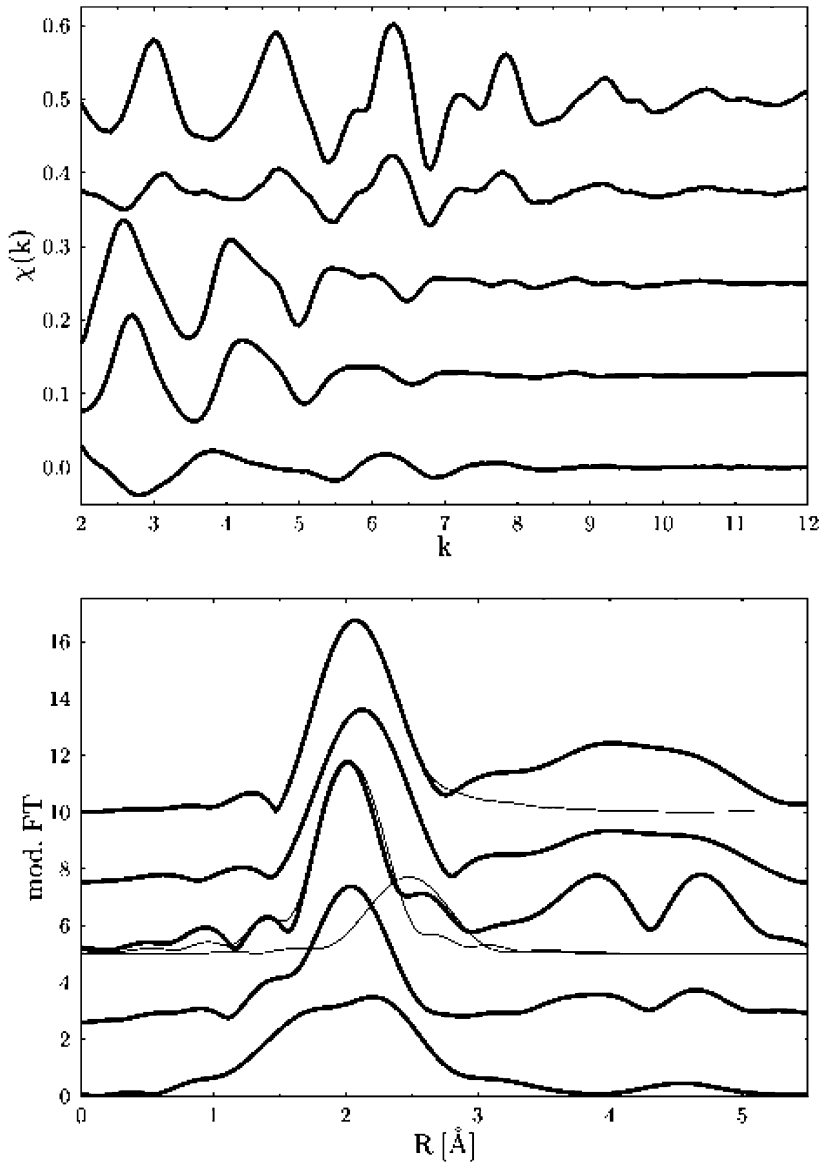

Figure 3. Mod. FT (lower panel) and chi (κ) functions (upper panel) for Ni, commercial Raney Ni, nanoscale NiAl, precursor, and new catalyst (top to bottom in each panel).

Both the Ni K-XANES and -EXAFS spectra of the nanoscopic NiAl reference and the precursor material are extremely similar to each other (see Figures 2 and 3a). The EXAFS analysis of the nanoscale NiAl (see Table 1) yields radial distances of 250 ± 2 pm (Ni−Al) and 286 ± 3 pm (Ni−Ni), which agree well with the structural information previously obtained from XRD-data.[17] The same is true for the relative coordination numbers of first-shell Al and second-shell Ni atoms, respectively, which scale as 8:6.7, whereas the absolute values obtained (5.1 ± 1 and 4.3 ± 1) are reduced compared to the bulk values. This might be assigned to the fact that one is dealing with agglomerates of individual particles with an average size of about 5 nm.[16] The results obtained from the analysis of the precursor data, which are also displayed in Table 1, yield similar distances (251 ± 2 pm and 289 ± 3 pm); the main difference consists of a change of the relative coordination numbers to 8:4.4, and a significant increase of the Debye−Waller factor. Both findings are expected. A number of authors have performed investigations on "classic" forms of Al-rich Raney catalysts before leaching and found mixtures consisting of local areas of NiAl, Ni_2Al_3, and pure Al as the main contributions,[13,14] explaining the increased degree of static disorder observed in the precursor material. Ni_2Al_3 itself can be described as a vacancy ordered phase of NiAl.[13] This fact explains the observed reduction of Ni−Ni coordination, which also appears plausible in an Al-rich phase.

Next, we will turn to the characterization of the spectra of the novel catalyst, which differ distinctly from those obtained for a conventional Raney Nickel catalyst. As discussed above, it is possible to assign the structures in the near-edge region of a compound to different types of bonds and/or bands using NiAl and Ni-lDOS provided in the "FEFF-8"-calculation. When looking at the Ni K-XANES spectrum of the novel catalyst, it is evident that resonance C is much stronger in comparison to the spectra of NiAl and the unleached precursor material (d vs e and f in Figure 2), indicating the presence of Ni−Ni bonds. At the same time, the multiple scattering structure D is hardly present at all, even weaker than in the spectrum of the commercial Raney Nickel catalyst, which indicates that any undisturbed Ni-coordination shell hardly is formed. This is due to the fact that Ni−Al bonds are still present in the system, as indicated by the steep increase in absorption on the low energy side of C due to the influence of resonance B and the missing minimum between structures D and F, which is due to

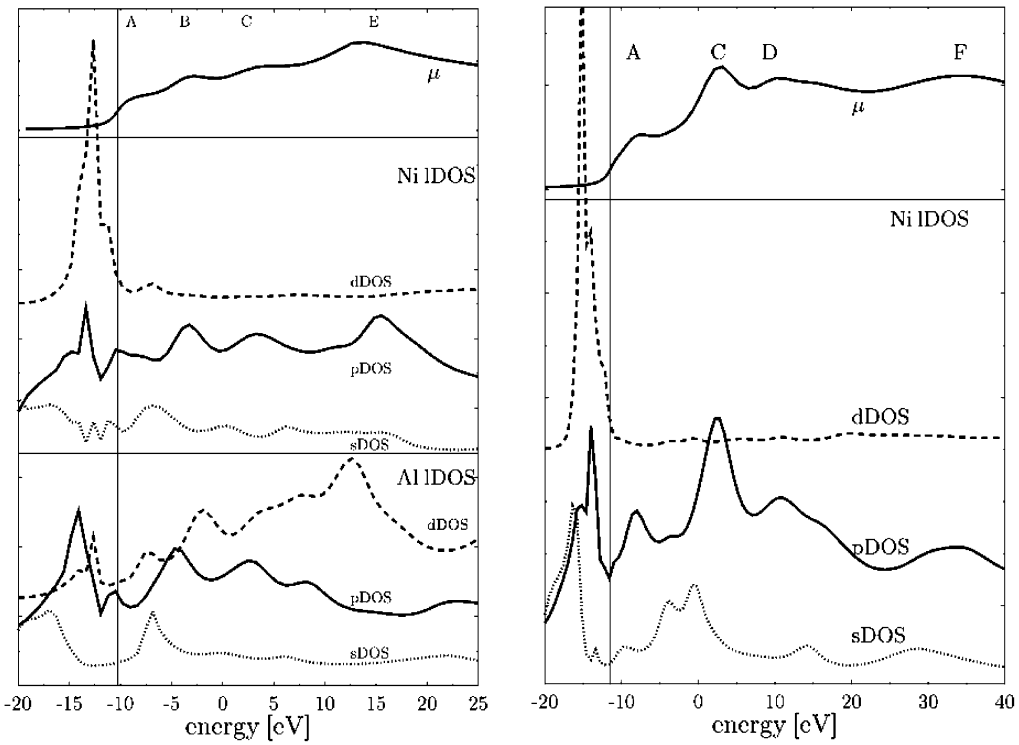

Figure 4. Calculations of atom- and l-projected DOS for (a) NiAl and (b) Ni foil, respectively.

TABLE 1: Coordination Number *N*, Interatomic Distance *R*, Debye−Waller Factor σ^2, and Edge Shift E_0 in eV Obtained from the EXAFS Analyses of the Samples

sample	path	N	*R* [pm]	σ^2	E_0
Ni	Ni−Ni	12 (fixed)	248 ± 1	0.006	−9.1
Raney Ni	Ni−Ni	6.6 ± 1	251 ± 2	0.007	−5.7
nano NiAl	Ni−Al	5.1 ± 1	250 ± 2	0.007	2.94
	Ni−Ni	4.3 ± 1	287 ± 3	0.015	2.94
precursor	Ni−Al	7.3 ± 1	251 ± 2	0.017	3.6
	Ni−Ni	4.3 ± 1	289 ± 3	0.037	8.9

contributions from the Ni−Al multiple scattering resonance E. Another indicator for the presence of Ni−Al bonds in the system is the slight shift of the position of structure A toward lower energies, which corresponds to the shift of the maximum of this structure toward lower energies for NiAl discussed above. A stronger onset of the absorption is also observed for the commercial Raney Nickel catalyst, which shows an increased intensity of structure A as compared to the Ni foil. This observation suggests that this effect is caused by vacancy positions in the lattice, which in turn shows that vacancy positions may also be present in the NiAl lattice.

This model for the structure of the new catalyst is also supported by a qualitative analysis of the EXAFS data displayed in Figure 4a,b. As mentioned above, in previous studies dealing with site-occupation tendencies in ternary β-phase transition metal aluminides,[37,38] a split double structure in the modified Fourier transform spectra has been established as a fingerprint indicator for the presence of a transition metal ion on Al sites in NiAl type material. This type of structure is reproduced only partly in our data, since, in contrast to the studies cited above, here the same transition metal atom is found on both sites in the lattice. Still it provides us with further evidence that the catalyst has retained a NiAl-structure in which a partial occupation of Al sites has occurred. Whereas in principle—neglecting the need to explain the observed enhancement of activity, which cannot be achieved using this approach—the XANES data might be reconciled with a phase mixture of NiAl and conventional Raney Nickel, the EXAFS data cannot be described as a superposition of these phase.

Despite the successful development of a qualitative model of the structure of the catalyst based on the XANES spectra of the catalyst and the calculations discussed above, it was not possible to use this model successfully in the frame of an EXAFS analysis to obtain a quantification of the observed changes. The reason for this is the degree of complexity needed to describe the system adequately. A nickel atom located on the Ni lattice space has a mixed first coordination shell composed of Ni and Al, both located at a distance of about 250 pm and a second coordination shell dominated by Ni atoms at about 286 pm. A nickel atom on an Al lattice space has a first coordination shell dominated by surrounding Ni atoms, but a mixed second coordination shell. On the basis of the available *k*-space, a stable and meaningful fit in this degree of complexity could not be achieved. A fit using just a Ni−Al and a Ni−Ni path yields distances which are in agreement with the distances in the precursor material, but the coordination numbers remain highly unstable, indicating that the two-path model is not sufficient to describe this material.

Summing up the accumulated structural information, it is possible to describe the structure of the novel catalyst in the framework of the NiAl lattice. Evidently, after the leaching process, one is dealing with a lattice in which Al sites have been partly occupied by Ni atoms and vancancies, but in which the removal of Al is evidently still incomplete. In fact, it is possible to correlate the differences between the structure of the leached catalyst and "classical" Raney Nickel to the special type of starting material used for its production. Several authors have discussed in detail the leaching process for Raney Nickel and correlated it to structural transitions occurring in the NiAl lattice of the starting material.[13−15] Such a structural transition within the crystal lattice is not possible for the nanocrystalline type of material we start from, as it requires long-range translational symmetry. In this scenario, it should also be expected that the removal of Al remains incomplete, as Ni-rich

NiAl phases are known to be rather insensitive toward the leaching reaction.

Conclusions

Detailed understanding of the electronic and geometric structure of a novel and highly active nanoscale skeletal nickel catalyst prepared via a "bottom up" route from nanoscale NiAl particles has been gained. In contrast to conventional Raney Nickel catalysts, this material can be described as a defect-rich structure within the NiAl lattice in which two types of defects are present: Al substitution by Ni and unoccupied Al-sites. The structural differences to standard leached Raney Nickel catalysts, especially the fact that a considerable number of Al atoms are not removed during the leaching process, are due to the nanoscopic nature of the starting material, which prevents the formation of a uniform reaction front in the material as well as structural transformations within the framework of an extended crystal lattice.

References and Notes

(1) Wainwright, M. S. In *Handbook of Heterogeneous Catalysis*; Knözinger, H, Ertl, G., Weitkamp, J., Eds.,; Wiley-VCH: Weinheim, 1977; p 64.

(2) Wainwright, M. S. In *Preparation of Solid Catalysists*; Ertl, G., Knözinger, H., Weitkamp, J., Eds.; Wiley-VCH: Weinheim, 1999; p 28.

(3) Klenke, B.; Gilbert, I. H. *J. Org. Chem.* **2001**, *66*, 2480.

(4) Couturier, M.; Tucker, J. L.; Andresen, B. M.; Dube, P.; Negri, J. T. *Org. Lett.* **2001,** *3*, 465.

(5) Franck-Neumann, M.; Geoffroy, P.; Bissinger, P.; Adelaide, S. *Tetrahedron Lett.* **2001**, *42*, 6401.

(6) Toth, M.; Somsak, L. *Tetrahedron Lett.* **2001**, *42*, 2723.

(7) Liu, B. J.; Lu, L. H.; Wang, B. C.; Cai, T. X. *Chin. J. Catal.* **2002**, *23*, 289.

(8) Al-Saleh, M. A.; Sleem-Ur-Rahman; Kareemuddin, S. M. M. J.; Al-Zakri, A. S. *J. Power Sources* **1998**, *72*, 159.

(9) Kukula, P.; Cerveny, L. *Appl. Catal. A* **2001**, *210*, 237.

(10) Kukula, P.; Cerveny, L. *J. Mol. Catal. A* **2002**, *185*, 195.

(11) Jobst, K.; Warlimont, H. *J. Catal.* **2002**, *207*, 23.

(12) Salmones, J.; Zeifert, B.; Cabanas-Moreno, J. B.; Aguilar-Rios, G.; Rojas, F.; Ramirez-Cuesta, A. *Adsorpt. Sci. Technol.* **2001**, *19*, 871.

(13) Wang, R.; Lu, Z. L.; Ko, T. *J. Mater. Sci.* **2001**, *36*, 5649.

(14) Knies, S.; Miehe, G.; Rettenmayr, M.; Ostgard, D. J. *Z. Metallkd.* **2001**, *92*, 596.

(15) Rothe, J.; Hormes, J.; Schild, C.; Pennemann B. *J. Catal.* **2000**, *191*, 294.

(16) Richards, R.; Geibel, G.; Hofstadt, W.; Bönnemann, H. *Appl. Organomet. Chem.* **2002**, *16*, 377.

(17) Bönnemann, H.; Brijoux, W.; Hofstadt, H. W.; Ould-Ely, T.; Schmidt, W.; Wassmuth, B.; Weidenthaler, C. *Angew. Chem.* **2002**, *41*, 599.

(18) Rothe, J.; Pollmann, J.; Franke, R.; Hormes, J.; Bönnemann, H.; Brijoux, W.; Siepen, K.; Richter, J. *Fresenius' J. Anal. Chem.* **1996**, *355*, 372.

(19) Bucher, S.; Hormes, J.; Modrow, H.; Brinkmann, R.; Waldöfner, N.; Bönnemann, H.; Beuermann, L.; Krischok, S.; Maus-Friedrichs, W.; Kempter, V. *Surf. Sci.* **2002**, *497*, 321.

(20) Angermund, K.; Bühl, M.; Dinjus, E.; Endruschat, U.; Gassner, F.; Hormes, J.; Köhl, G.; Mauschick, F. T.; Modrow, H.; Mörtel, R.; Mynott, R.; Tesche, B.; Waldöfner, N.; Bönnemann, H. *Angew. Chem., Int. Ed.* **2002**, *41*, 4041.

(21) Teo, B. K. *EXAFS: Basic Principles and Data Analysis, Inorg. Chem. Concepts*; Springer: Berlin, 1986.

(22) Vairavamurthy, A. *Spectrochim. Acta A* **1998**, *54*, 2009.

(23) Hu, Z.; Kaindl, G.; Meyer, G. *J. Alloys Compd.* **1998**, *274*, 38.

(24) Hu, Z.; Mazundar, C.; Kaindl, G.; de Groot, F. M. F.; Warda, S. A.; Reinen, D. *Chem. Phys. Lett.* **1998**, *297*, 321.

(25) Iwanowski, R. J.; Lawniczak-Jablonska, K. *Acta Phys. Pol., A* **1997**, *97*, 803.

(26) Pantelouris, A.; Modrow, H.; Pantelouris, M.; Hormes, J.; Reinen, D. *Chem. Phys*., accepted.

(27) Modrow, H.; Zimmer, R.; Viesel, F.; Hormes, J. *Rubber Chem. Technol.* **2001**, *74*, 281.

(28) Prange, A.; Chauvistré, R.; Modrow, H.; Hormes, J.; Trüper, H. G.; Dahl, C. *Microbiology UK* **2002**, *148*, 267.

(29) Modrow, H.; Bucher, S.; Ankudinov, A.; Rehr, J. J. *Phys. Rev. B* **2003**, 035123.

(30) Gilbert, B.; Frazer, B. H.; Belz, A.; Conrad, P. G.; Nealson, K. H.; Haskel, D.; Lang, J. C.; Srajer, G.; De Stasio, G. *J. Phys. Chem. A* **2003**, *107*, 2839.

(31) Lemonnier, M.; Collet, O.; Depautex, C.; Esteva, J. M.; Raoux, D. *Nucl. Instrum. Methods* **1978**, *152*, 109.

(32) Thompson, A., et al. *X-ray Data Booklet;* LBNL/Pub-490 Rev.2.

(33) Stern, E. A.; Newville, M.; Ravel, B.; Yacoby, Y.; Haskel, D. *Physica B* **1995**, *209*, 117.

(34) Newville, M.; Livins, P.; Yacoby, Y.; Rehr, J. J.; Stern, E. A. *Phys. Rev. B* **1993**, *47*, 14126.

(35) Newville, M.; Ravel, B.; Haskel, D.; Stern, E. A.; Yacoby, Y. *Physica B* **1995**, *209*, 145.

(36) Ankudinov, A. L.; Ravel, B.; Rehr, J. J.; Conradson, S. D. *Phys. Rev. B* **1998**, *58*, 7565.

(37) Chartier, P.; Balasubramanian, M.; Brewe, D. L.; Manzur, T.; Pease, D. M.; Budnick, J. I.; Huang, L.; Law, C.; Russell, S.; Kimball, C. *J. Appl. Phys.* **1994**, *75*, 3842.

(38) Balasubramanian, M.; Pease, D. M.; Budnick, J. I.; Manzur, T.; Brewe, D. L.; *Phys. Rev. B* **1995**, *51*, 8102.

(39) Frenzel, B.; Rothe, J.; Hormes, J.; Fornasisni, P. *J. Phys. IV France* **1997**, *7*, C2−273.

(40) Nakabayashi, I.; Nagao, E.; Miyata, K.; Moriga, T.; Ashida, T.; Tomida, T.; Hyland, M.; Meston, J. *J. Mater. Chem.* **1995**, *5*, 737.